

POLYAK-VIRO TYPE FORMULA FOR THE MILNOR TRIPLE LINKING NUMBER OF LINK DIAGRAMS WITH MULTIPLE-CROSSINGS

YUSAKU OKUHARA AND KEIICHI SAKAI

ABSTRACT. We obtain Polyak-Viro type formula for the Milnor triple linking number that can be applied to diagrams with triple or more multiple-crossings. The proof is based on the idea of Brooks and Komendarczyk [4], but is different from theirs in that we explicitly compute the value of configuration space integral associated to the “Y-graph,” and is applicable to the original Brooks-Komendarczyk formula for the Casson knot invariant. The results for the Milnor triple linking number were firstly obtained in the first author’s master thesis, in which the proof follows the same way as that in [4].

1. INTRODUCTION

Configuration space integral [1, 3, 5, 6, 13] provides us a systematic way to express all the Vassiliev invariants for (long) knots and links. It also enables us to compute Vassiliev invariants in combinatorial ways; the Polyak-Viro type formulas [9, 10] can be deduced from configuration space integrals. Moreover it motivates us to think of invariants for high dimensional embeddings as generalizations of Vassiliev invariants, see for example [11, 12, 14].

Robyn Brooks and Rafal Komendarczyk [4] got an idea to replace the standard volume form of S^2 with a 2-form whose support is localized to a neighborhood of a point (say the north pole). This idea can work well only for the Vassiliev invariants of order two, but extremely simplifies the computation of configuration space integral since, with such a 2-form, the integrals “localize” to neighborhoods of crossings of knot diagrams and get to be computable in a combinatorial way. Indeed Brooks and Komendarczyk were able to deduce Polyak-Viro type formula for the *Casson knot invariant* that is applicable to diagrams with triple or more multiple crossings. They firstly proved the original Polyak-Viro formula for the Casson invariant [10] using configuration space integral, and then addressed the case of diagrams with multiple crossings by resolving the multiple crossings into ordinary double crossings to apply the original Polyak-Viro formula. Such resolutions allow us to avoid the computation of configuration space integral associated to the “Y-graph” (see Figure 3.3 below).

In this paper we give a similar combinatorial formula for the *Milnor triple linking number* of 3-component long links (Theorem 2.6). The proof is different from that in [4] in that we explicitly compute the Y-graph integral. Our computation clarifies the nature of the Y-graph as a “correction term” to some extent. Our method can also be applied to reprove the formula in [4], and might be useful for further study of Vassiliev invariants of order two.

The paper is organized as follows. In §2 we introduce arrow / Gauss diagrams that are needed to state our main results (Theorem 2.6). §3 describes three invariants using configuration space integrals; the linking number for 2-component links, the Casson knot invariant, and the Milnor triple linking number. We review the integral expression of the linking numbers of 2-component links for two reasons. One is that the linking number can be seen as the simplest example of configuration space integrals, and the other is that we obtain a “localizing technique” of integrations through an explicit computation of the linking number. In §4 we give the proof of the main results by computing configuration space integrals in the case where diagrams have multiple crossings.

ACKNOWLEDGMENTS

The authors would like to express their great appreciation to Robyn Brooks and Rafal Komendarczyk for helpful comments and suggestions. The second author was partially supported by JSPS KAKENHI Grant Numbers 20K03608 and 23K20795.

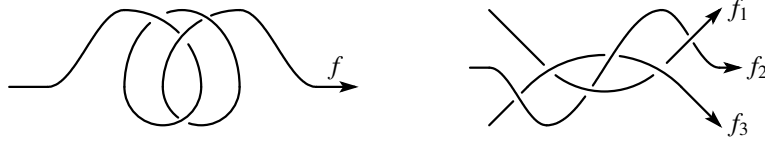


FIGURE 2.1. Long knot and 3-component long link

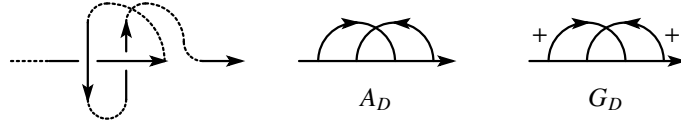


FIGURE 2.2. Examples of arrow / Gauss diagrams for double crossings

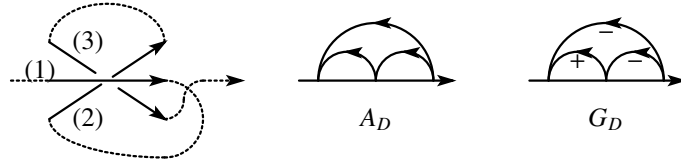


FIGURE 2.3. Examples of arrow / Gauss diagrams for triple crossings; the arc (2) is front of (3)

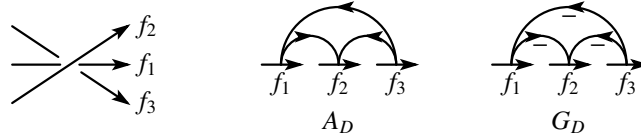


FIGURE 2.4. Examples of arrow / Gauss diagrams for triple crossings; the three arcs are contained in mutually distinct components of a 3-component link, and the arc of f_1 is front of that of f_3

2. PRELIMINARIES AND THE MAIN RESULTS

Definition 2.1. A *long knot* in \mathbb{R}^3 is an embedding $f: \mathbb{R}^1 \hookrightarrow \mathbb{R}^3$ that satisfies $f(x) = (x, 0, 0)$ if $|x| \geq 1$. A *3-component long link* in \mathbb{R}^3 is an embedding $f = f_1 \sqcup f_2 \sqcup f_3: \mathbb{R}^1 \sqcup \mathbb{R}^1 \sqcup \mathbb{R}^1 \hookrightarrow \mathbb{R}^3$ that satisfies $f_k(x) = (x, (2-k)|x|, 0)$ if $|x| \geq 1$. See Figure 2.1.

Let $N = (0, 0, 1) \in \mathbb{R}^3$, and let N^\perp be the 2-dimensional subspace of \mathbb{R}^3 perpendicular to N . We denote the projection from \mathbb{R}^3 onto N^\perp (resp. $\mathbb{R}N$) by pr_{12} (resp. pr_3).

In this paper, unless otherwise stated, a *diagram* of a (long) knot or link f in \mathbb{R}^3 is the projection of f onto N^\perp with over / under information, that may have *transverse multiple crossings*. Namely, $\text{pr}_{12}(f)$ may go through a point twice or more times, but all the tangent vectors at the point should generate mutually different lines.

Remark 2.2. We think of a multiple crossing as consisting of several fewer multiple crossings; for example, a triple crossing consists of three double crossings, and a quadruple crossing contains four triple crossings and six double crossings.

Let f be a long knot with a diagram D . The *arrow diagram* A_D for D is the set of ordered pairs (t_i, u_i) ($i = 1, 2, \dots$) of real numbers, where each (t_i, u_i) corresponds to a double crossing $\text{pr}_{12}(f(t_i)) = \text{pr}_{12}(f(u_i))$ of D with $\text{pr}_3(f(t_i)) < \text{pr}_3(f(u_i))$. We depict A_D as a graph that has vertices t_i and u_i ($i = 1, 2, \dots$) on \mathbb{R}^1 with oriented chords emanating from t_i to u_i (see Figures 2.2, 2.3). The *Gauss diagram* G_D is A_D with the signs of the double crossings of D attached to corresponding chords.

The *3-strand arrow diagram* and the *3-strand Gauss diagram* of a diagram D of a 3-component long link are defined in the same way. It is a union of three copies of \mathbb{R}^1 with vertices on these \mathbb{R}^1 's connected by oriented chords corresponding to double crossings (and the signs of these crossings are attached to these chords, see Figure 2.4).

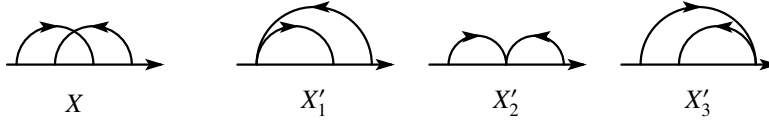


FIGURE 2.5. Arrow diagrams X and X'_k ($k = 1, 2, 3$)

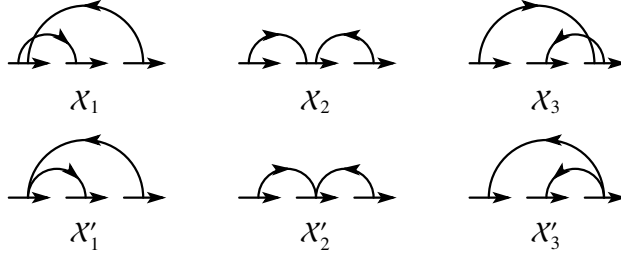


FIGURE 2.6. Arrow diagrams X_k and X'_k ($k = 1, 2, 3$)

Definition 2.3. For a diagram D of a long knot, let $C^2(D)$ the set of unordered pairs (α, β) of chords α, β of A_D . Let X and X'_k , $k = 1, 2, 3$, be the arrow diagrams as shown in Figure 2.5, and define

$$(2.1) \quad C_*^2(D) := \{(\alpha, \beta) \in C^2(D) \mid \alpha \text{ and } \beta \text{ form a subdiagram of } A_D \text{ that is isomorphic to } *\}, \quad * = X, X'_1, X'_2 \text{ or } X'_3.$$

Then define

$$(2.2) \quad \langle X, G_D \rangle := \sum_{(\alpha, \beta) \in C_X^2(D)} \text{sgn}(\alpha)\text{sgn}(\beta), \quad \langle X'_k, G_D \rangle := \sum_{(\alpha, \beta) \in C_{X'_k}^2(D)} \text{sgn}(\alpha)\text{sgn}(\beta),$$

where $\text{sgn}(\alpha) \in \{+1, -1\}$ is the sign of α seen as a chord of G_D .

Let c denote the *Casson invariant* of (long) knots, namely the coefficient of the quadratic term of the Alexander-Conway polynomial. Brooks and Komendarczyk [4] gave a combinatorial formula that computes the value of c from (long) knot diagrams possibly with multiple crossings.

Theorem 2.4 ([4, Theorem A, B], see also [10, Theorem 1]). *If a diagram D of a long knot f has only transverse double crossing, then*

$$(2.3) \quad c(f) = \langle X, G_D \rangle.$$

For a general diagram D of a long knot f , we have

$$(2.4) \quad c(f) = \langle X, G_D \rangle + \frac{1}{2} (\langle X'_1, G_D \rangle + \langle X'_2, G_D \rangle + \langle X'_3, G_D \rangle).$$

Our main results are analogous formulas to (2.3) and (2.4) for the *Milnor triple linking number* [?].

Definition 2.5. For a diagram D of a 3-component long link f , let $C^2(D)$ be defined in the same way as in Definition 2.3. Let X_k and X'_k , $k = 1, 2, 3$, be the arrow diagrams as shown in Figure 2.6, and define

$$(2.5) \quad C_*^2(D) := \{(\alpha, \beta) \in C^2(D) \mid \alpha \text{ and } \beta \text{ form a subdiagram of } A_D \text{ that is isomorphic to } *\}, \quad * = X_k \text{ or } X'_k \text{ (} k = 1, 2, 3\text{)}.$$

Then define

$$(2.6) \quad \langle X_k, G_D \rangle := \sum_{(\alpha, \beta) \in C_{X_k}^2(D)} \text{sgn}(\alpha)\text{sgn}(\beta), \quad \langle X'_k, G_D \rangle := \sum_{(\alpha, \beta) \in C_{X'_k}^2(D)} \text{sgn}(\alpha)\text{sgn}(\beta).$$

Theorem 2.6. *If a diagram D of a 3-component long link f has only transverse double crossing, then*

$$(2.7) \quad \mu(f) = \langle X_1, G_D \rangle + \langle X_2, G_D \rangle + \langle X_3, G_D \rangle.$$

For a general diagram D of a 3-component long link f , we have

$$(2.8) \quad \mu(f) = \langle X_1, G_D \rangle + \langle X_2, G_D \rangle + \langle X_3, G_D \rangle + \frac{1}{2} (\langle X'_1, G_D \rangle + \langle X'_2, G_D \rangle + \langle X'_3, G_D \rangle).$$

Remark 2.7. (2.7) has already been known as [?, Theorem 3], proved in a different way from ours.

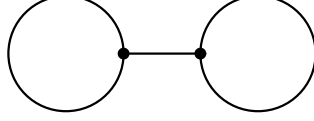


FIGURE 3.1. The graph that corresponds to the linking number

3. CONFIGURATION SPACE INTEGRAL AND THE POLYAK FORMULA FOR THE MILNOR TRIPLE LINKING NUMBER

Configuration space integral is firstly introduced in [3, 6] to produce all the Vassiliev invariants for knots from appropriate formal sums of trivalent graphs, and then generalized in [5, 8] to give cochain maps (up to some correction terms) from graph complexes to de Rham complex of the spaces of (long) knots and links. In this paper we only give the constructions of the linking number, the Casson knot invariant and the Milnor triple linking number. See also [1, 7, 13] for general construction.

3.1. The linking number of 2-component links. For simplicity, we treat with ordinary 2-component links, namely embeddings $f: S^1 \sqcup S^1 \hookrightarrow \mathbb{R}^3$.

For a 2-component link $f = (f_1, f_2)$, define a map

$$(3.1) \quad h = h_f: S^1 \times S^1 \rightarrow S^2, \quad h(x_1, x_2) := \frac{f_2(x_2) - f_1(x_1)}{|f_2(x_2) - f_1(x_1)|}.$$

Then the linking number of f , the mapping degree of h , is given by

$$(3.2) \quad \text{link}(f) := \int_{S^1 \times S^1} h^* \eta,$$

here η is a ‘‘Dirac-like’’ 2-form $\eta = \eta_\epsilon^N \in \Omega_{dR}^2(S^2)$ that satisfies

- (i) $\text{supp}(\eta)$ is contained in the ϵ -neighborhood of the north pole $N = (0, 0, 1) \in \mathbb{R}^3$,
- (ii) η is invariant under the action of $O(2) = O(2) \times \{\text{id}\} \subset O(3)$ (namely $\varphi^* \eta = (-1)^{\det \varphi} \eta$ for $\varphi \in O(2)$), and
- (iii) η is a unit 2-form, that is, $\int_{S^2} \eta = 1$.

The construction (3.2) is encoded by the graph shown in Figure 3.1; we consider $S^1 \times S^1$, thought of as ‘‘two-point configuration space on S^1 ,’’ associated to the two vertices on the circles (one on each component), and also consider the map h associated to the edge connecting these two vertices.

The integral (3.2) is independent of the choice of non-exact unit 2-forms of S^2 . Following [4] we choose η , that simplifies computations of the integrals as we see in Example 3.1 below. In fact, we do not need to impose the assumption (ii) to define the linking number; we need it only for the Milnor triple linking number.

Example 3.1. Let $f = (f_1, f_2)$ be the Hopf link (see Figure 3.2), and suppose a diagram D of f has exactly two crossings p and q with f_2 being the over-arc at $p = \text{pr}_{12}(f_1(t)) = \text{pr}_{12}(f_2(u))$. If the radius $\epsilon > 0$ of $\text{supp}(\eta)$ is sufficiently close to 0, then $h(x_1, x_2) \in \text{supp}(\eta)$ only if x_1 and x_2 are near t and u respectively. Thus there exist neighborhoods U and V of t and u such that

$$(3.3) \quad \text{link}(f_1, f_2) = \int_{U \times V} h^* \eta.$$

Since $\text{link}(f_1, f_2)$ is equal to the sign of p , we have

$$(3.4) \quad \int_{U \times V} h^* \eta = \text{sgn}(p).$$

Hereafter we consider similar integrals to (3.2) associated to other arrow diagrams or graphs. Since we use η , in many cases such integrals ‘‘localize’’ to those near the crossing points, and then (3.4) converts the computation of the integrals to a combinatorics, namely a counting of certain kinds of crossings.

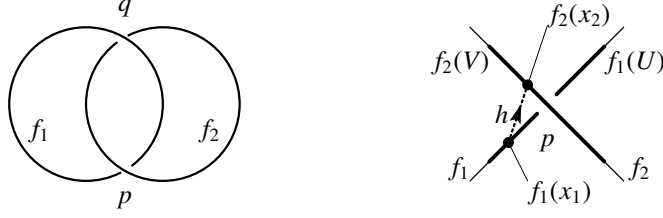


FIGURE 3.2. The Hopf link

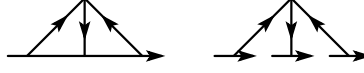


FIGURE 3.3. The graphs Y and \mathcal{Y}

3.2. The Casson invariant for long knots. Let f be a long knot. Associated to X (Figure 2.5), consider the configuration space

$$(3.5) \quad C_X := \{(x_1, \dots, x_4) \in (\mathbb{R}^1)^{\times 4} \mid x_1 < \dots < x_4\}$$

and the maps $h_{13}, h_{42}: C_X \rightarrow S^2$ defined by

$$(3.6) \quad h_{ij}(x_1, \dots, x_4) := \frac{f(x_j) - f(x_i)}{|f(x_j) - f(x_i)|}, \quad (i, j) = (1, 3), (4, 2).$$

We remark that these maps are obviously defined as indicated by the oriented chords of X (Figure 2.5). We put $h_X := h_{13} \times h_{42}: C_X \rightarrow (S^2)^{\times 2}$ for simplicity, and consider the (possibly diverging) integral

$$(3.7) \quad I_X(f) := \int_{C_X} \omega_X, \quad \omega_X := h_X^*(\eta \times \eta).$$

Next, associated to the graph Y (Figure 3.3, the left), consider the configuration space

$$(3.8) \quad C_Y(f) := \{(x_1, x_2, x_3, x_4) \in (\mathbb{R}^1)^{\times 2} \times \mathbb{R}^3 \mid f(x_i) \neq x_4, i = 1, 2, 3\},$$

and the maps $h_{i4}: C_Y(f) \rightarrow S^2$ ($i = 1, 3$) and $h_{42}: C_Y(f) \rightarrow S^2$ defined by

$$(3.9) \quad h_{i4}(x_1, x_2, x_3, x_4) := \frac{x_4 - f(x_i)}{|x_4 - f(x_i)|} \quad (i = 1, 3), \quad h_{42}(x_1, x_2, x_3, x_4) := \frac{f(x_2) - x_4}{|f(x_2) - x_4|}.$$

These maps are also defined as indicated by the oriented chords of Y . We put $h_Y := h_{14} \times h_{42} \times h_{34}: C_Y(f) \rightarrow (S^2)^{\times 3}$ and define

$$(3.10) \quad I_Y(f) := \int_{C_Y(f)} \omega_Y, \quad \text{where } \omega_Y := h_Y^*(\eta \times \eta \times \eta).$$

Proposition 3.2. *The integrals $I_X(f)$ and $I_Y(f)$ converge.*

Proof. The Axelrod-Singer compactifications [2] of $C_X(f)$ and $C_Y(f)$ are manifolds with corners, onto which the maps h_{ij} are smoothly extended. Thus ω_X and ω_Y are defined on the compactified configuration spaces, and their integrals converge. \square

Theorem 3.3 ([3, 6, 4]). *$I_X(f) - I_Y(f)$ is an invariant for long knots and is equal to the Casson invariant $c(f)$ of f .*

Theorem 3.3 can be proved in the same way as in [3, 6], but we have to pay attention to the choice of the volume form η .

Indeed, (3.7) and (3.10) give rise to 0-forms on the space of long knots. By the Stokes' theorem (that is generalized so that it can be applied to integrations along the fiber), the exterior differentials of the 0-forms I_* ($* = X, Y$) are

$$(3.11) \quad dI_* = \int_{C_*} d\omega_* \pm \int_{\partial C_*} \omega_* = \pm \int_{\partial C_*} \omega_*.$$

The boundary of (compactified) C_X is stratified, and each codimension one (open) stratum consists of the configurations (x_1, x_2, x_3, x_4) such that

- (i) exactly two x_i 's collide,
- (ii) three or more x_i 's collide, or
- (iii) some of x_i "escape to infinity" (or "collide with the point at infinity").

It can be shown that the integrations over the strata of types (ii) and (iii) vanish, by dimensional reasons (see for example [5, Appendix A]). Thus dI_X is equal to the sum of integrals over the type (i) strata. The situation is similar for Y , and the type (i) contributions for X and Y cancel to each other because the formal sum $X - Y$ is a "graph cocycle" with respect to the coboundary map defined as the signed sum of the edge-contractions. Thus we show that $c := I_X - I_Y$ is a closed 0-form on the space of long knots, that is, an isotopy invariant. Indeed c is the Casson invariant, because c satisfies (2.3) that is equal to the formula for the Casson invariant given in [10].

For general graphs Z other than X and Y , the boundary of the (compactified) C_Z has other types of strata, where three or more points collide. If we use a volume form that is invariant with respect to the antipodal map $S^2 \rightarrow S^2$, then almost all the integrals over such strata turns out to vanish, by a "symmetry argument" (see for example [5, Appendix A]). Our η is not symmetric and these arguments might fail. Moreover there exists one more type of strata, the *anomalous strata*, where all the points collide simultaneously. It is not known whether the integrals over the anomalous strata vanish or not for general graphs, and we need to add some correction terms. Fortunately, for both X and Y , such symmetry arguments as above are not necessary, and the contribution of the anomalous strata can be shown to vanish by dimensional reasons.

3.3. The Milnor triple linking number. Let $f = f_1 \sqcup f_2 \sqcup f_3$ be a 3-component long link. Associated to X_1 (Figure 2.6), consider the configuration space

$$(3.12) \quad C_{X_1} := \{(x_1, x_2), x_3, x_4) \in (\mathbb{R}^1)^{\times 2} \times \mathbb{R}^1 \times \mathbb{R}^1 \mid x_1 < x_2\}.$$

We think of $((x_1, x_2), x_3, x_4) \in C_{X_1}$ as a quadruple of points on f , with x_1, x_2 on f_1 , x_3 on f_2 and x_4 on f_3 . Define the maps $h_{13}, h_{42}: C_{X_1} \rightarrow S^2$ as indicated by the oriented chords of X_1 (Figure 2.6);

$$(3.13) \quad h_{13}(x_1, \dots, x_4) := \frac{f_2(x_3) - f_1(x_1)}{|f_2(x_3) - f_1(x_1)|}, \quad h_{42}(x_1, \dots, x_4) := \frac{f_3(x_4) - f_1(x_2)}{|f_3(x_4) - f_1(x_2)|}.$$

We put $h_{X_1} := h_{13} \times h_{42}: C_{X_1} \rightarrow (S^2)^{\times 2}$ and define

$$(3.14) \quad I_{X_1}(f) := \int_{C_{X_1}} \omega_{X_1}, \quad \text{where } \omega_{X_1} := h_{X_1}^*(\eta \times \eta).$$

Similarly, associated to X_2 and X_3 (Figure 2.6), consider the configuration spaces

$$(3.15) \quad C_{X_2} := \{(x_1, (x_2, x_3), x_4) \in \mathbb{R}^1 \times (\mathbb{R}^1)^{\times 2} \times \mathbb{R}^1 \mid x_2 < x_3\},$$

$$(3.16) \quad C_{X_3} := \{(x_1, x_2, (x_3, x_4)) \in \mathbb{R}^1 \times \mathbb{R}^1 \times (\mathbb{R}^1)^{\times 2} \mid x_3 < x_4\},$$

and define the maps $h_{12}, h_{43}: C_{X_2} \rightarrow S^2$ and $h_{13}, h_{42}: C_{X_3} \rightarrow S^2$ as indicated by the oriented chords of X_2 and X_3 (Figure 2.6). We put $h_{X_2} := h_{12} \times h_{43}: C_{X_2} \rightarrow (S^2)^{\times 2}$ and $h_{X_3} := h_{13} \times h_{42}: C_{X_3} \rightarrow (S^2)^{\times 2}$, and define

$$(3.17) \quad I_{X_k}(f) := \int_{C_{X_k}} \omega_{X_k}, \quad \text{where } \omega_{X_k} := h_{X_k}^*(\eta \times \eta) \quad (k = 2, 3).$$

Finally, associated to the graph \mathcal{Y} (Figure 3.3, the right), consider the configuration space

$$(3.18) \quad C_{\mathcal{Y}}(f) := \{(x_1, x_2, x_3; x_4) \in (\mathbb{R}^1)^{\times 3} \times \mathbb{R}^3 \mid f_k(x_k) \neq x_4 \ (k = 1, 2, 3)\}$$

and define the maps $h_{i4}: C_{\mathcal{Y}}(f) \rightarrow S^2$ ($i = 1, 3$) and $h_{42}: C_{\mathcal{Y}}(f) \rightarrow S^2$ as indicated by the oriented chords of \mathcal{Y} (Figure 3.3). We put $h_{\mathcal{Y}} := h_{14} \times h_{42} \times h_{34}: C_{\mathcal{Y}}(f) \rightarrow (S^2)^{\times 3}$ and define

$$(3.19) \quad I_{\mathcal{Y}}(f) := \int_{C_{\mathcal{Y}}(f)} \omega_{\mathcal{Y}}, \quad \text{where } \omega_{\mathcal{Y}} := h_{\mathcal{Y}}^*(\eta \times \eta \times \eta).$$

Proposition 3.4. *The integrals $I_{X_k}(f)$ ($k = 1, 2, 3$) and $I_{\mathcal{Y}}(f)$ converge.*

This is because, similar to Proposition 3.2, the Axelrod-Singer compactifications [2] for C_{X_k} ($k = 1, 2, 3$) and $C_{\mathcal{Y}}$ also exist.

Theorem 3.5 ([7]). *$\mu(f) := I_{X_1}(f) + I_{X_2}(f) + I_{X_3}(f) - I_{\mathcal{Y}}(f)$ is equal to the Milnor triple linking number $\mu_{123}(f)$ of f .*

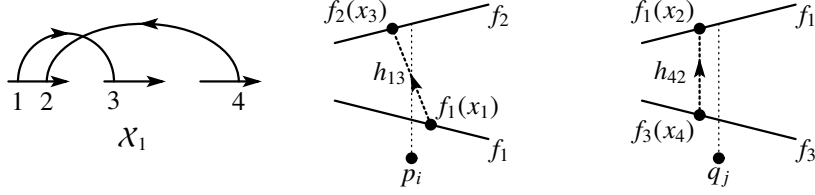


FIGURE 3.4.

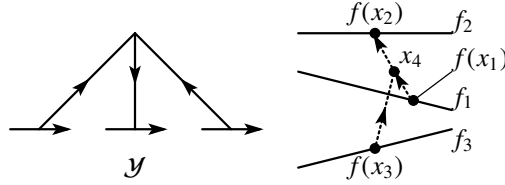


FIGURE 3.5.

The proof of Theorem 3.5 is the same as that in [7]. Similarly to the case of the Casson invariant, we need to check that no symmetry argument is needed. The proof is easier in this case than in the case of the Casson invariant; there exist no anomalous faces for \mathcal{X}_k 's and \mathcal{Y} . This is because not all the four configuration points are on a single component and hence not all of them can collide.

3.4. Proof of (2.7), the first half of Theorem 2.6. The Polyak formulas (2.3) and (2.7) can be proved in parallel ways, so we only give a proof of (2.7). The proof below almost repeats verbatim that for (2.3) in [4].

Let us compute $I_{\mathcal{X}_1}(f)$ for a 3-component long link f whose projection onto N^\perp is a usual link diagram D , namely D has only transverse double crossings.

Let p_1, p_2, \dots be the crossings of D that involve f_1 and f_2 with arcs of f_2 as the over-arcs. Similarly let q_1, q_2, \dots be the crossings of D that involve f_1 and f_3 with arcs of f_1 as their over-arcs. Suppose $p_i = \text{pr}_{12}(f_1(t_i)) = \text{pr}_{12}(f_3(u_i))$ and $q_j = \text{pr}_{12}(f_1(t'_j)) = \text{pr}_{12}(f_2(u'_j))$. Then, if ϵ is sufficiently close to 0, the image $h_{\mathcal{X}_1}((x_1, x_2), x_3, x_4)$ of $((x_1, x_2), x_3, x_4) \in C_{\mathcal{X}_1}$ via the map $h_{\mathcal{X}_1}$ (the product of the maps in (3.13)) is in $\text{supp}(\eta)^{\times 2}$ only if x_1 and x_3 are near respectively t_i and u_i for some i , and x_2 and x_4 are near respectively t'_j and u'_j for some j , with $t_i < t'_j$ (Figure 3.4). Thus, there exist disjoint neighborhoods U_i^1, U_i^3, V_j^2 and V_j^4 of respectively t_i, u_i, t'_j and u'_j such that

$$(3.20) \quad \lim_{\epsilon \rightarrow 0} I_{\mathcal{X}_1}(f) = \sum_{\substack{i,j \\ t_i < t'_j}} \int_{U_i^1 \times V_j^2 \times U_i^3 \times V_j^4} \omega_{\mathcal{X}_1} = \sum_{\substack{i,j \\ t_i < t'_j}} \int_{U_i^1 \times U_i^3} h_{13}^* \eta \int_{V_j^2 \times V_j^4} h_{42}^* \eta,$$

here we permute the coordinates as $(x_2, x_3, x_4) \mapsto (x_3, x_4, x_2)$, whose sign is $+1$. The integrations in the most right hand side of (3.20) are nothing but the right hand side of (3.3) in Example 3.1, and are equal to the signs of the crossings p_i and q_j . The chords corresponding to p_i and q_j with $t_i < t'_j$ obviously form a subdiagram of G_D isomorphic to \mathcal{X}_1 . Thus

$$(3.21) \quad \lim_{\epsilon \rightarrow 0} I_{\mathcal{X}_1}(f) = \sum_{\substack{i,j \\ t_i < t'_j}} \text{sgn}(p_i) \text{sgn}(q_j) = \langle \mathcal{X}_1, G_D \rangle.$$

In the same way we see that

$$(3.22) \quad \lim_{\epsilon \rightarrow 0} I_{\mathcal{X}_k}(f) = \langle \mathcal{X}_k, G_D \rangle, \quad k = 2, 3.$$

As for \mathcal{Y} , the image of $(x_1, x_2, x_3; x_4) \in C_{\mathcal{Y}}(f)$ via $h_{\mathcal{Y}}$ is in $(\text{supp}(\eta))^{\times 3}$ only if

- $\text{pr}_{12}(f_i(x_i))$ ($i = 1, 2, 3$) and $\text{pr}_{12}(x_4)$ are sufficiently near, and
- $f_i(x_i)$ sits “below” (resp. “above”) x_4 if $i = 1, 3$ (resp. $i = 2$)

(see Figure 3.5). Thus $\text{supp}(\omega_{\mathcal{Y}})$ is contained in the subspace of $(x_1, x_2, x_3; x_4) \in C_{\mathcal{Y}}(f)$ with $f_i(x_i)$ ($i = 1, 2, 3$) “near a triple point of the diagram D ”, and is empty if ϵ is sufficiently small, since D has no triple point. This implies

$$(3.23) \quad \lim_{\epsilon \rightarrow 0} I_{\mathcal{Y}}(f) = 0.$$

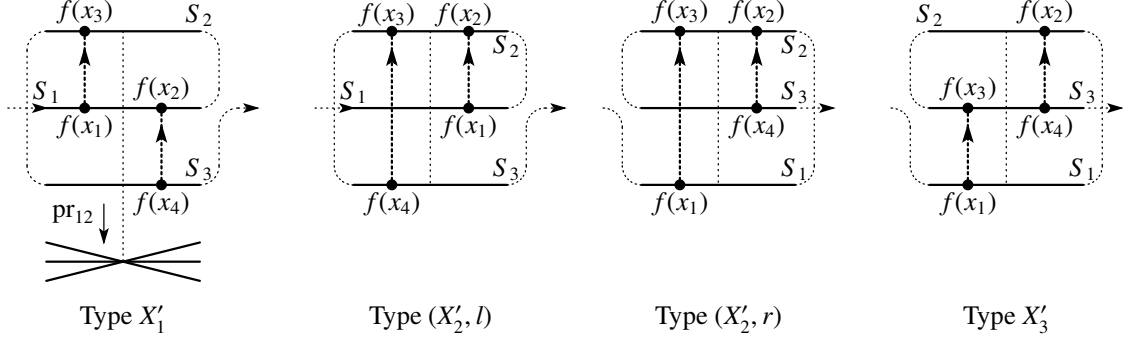


FIGURE 4.1. Configurations that can contribute to I_X and I_{X_k}

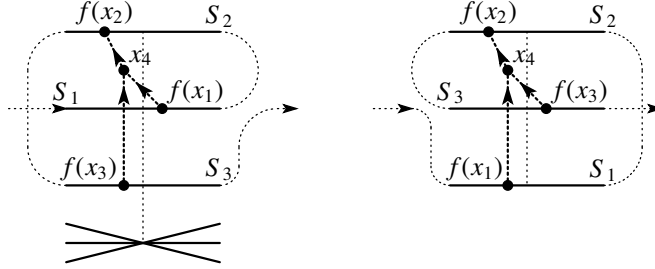


FIGURE 4.2. Configurations that can contribute to I_Y and I_Y

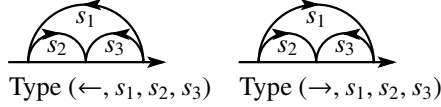


FIGURE 4.3. All possible Gauss diagrams for triple points that can contribute to I_X and I_Y ($s_1, s_2, s_3 \in \{+, -\}$)

(3.21), (3.22) and (3.23) complete the proof of (2.7).

Almost the same argument proves (2.3), just replacing \mathcal{X}_k and \mathcal{Y} respectively with X_k and Y .

4. POLYAK TYPE FORMULA FOR MILNOR TRIPLE LINKING NUMBER FROM LINK DIAGRAMS WITH MULTIPLE CROSSINGS

Below we suppose that diagrams of long knots and links may have transverse multiple (triple or more) crossings. The pairs of double crossings that do not form triple or quadruple points contribute to the Casson invariant and the Milnor triple linking number by the product of the signs of these crossings, as we see in §3.4. In this case triple or more crossings may also contribute to these invariants, because $\text{supp}(\omega_*)$ contains configurations as shown in Figures 4.1, 4.2, where all the four points get together near a triple point. We compute these contributions in the limit $\epsilon \rightarrow 0$.

4.1. A “model” for triple points. Consider three disjoint small straight segments S_1, S_2 and S_3 in \mathbb{R}^3 that are parallel to N^\perp and whose projections onto N^\perp make a transverse triple point at their midpoints. We regard these segments as

- subarcs of a long knot f such that, if we follow f along its orientation, we pass through these segments in order of S_1, S_2 and then S_3 , or
- subarcs of a long link f with S_k on the k -th component f_k ($k = 1, 2, 3$) of f .

To compute the contribution of triple points to I_X and I_{X_k} , we will consider configurations of four points on the segments S_k and the maps h_{ij} defined similarly to (3.6) and (3.13), then compute the integral defined similarly to (3.7) and (3.14). The contribution of triple points to I_Y and I_Y will be computed in similar way.

We only need to consider the case where S_2 is “above” both S_1 and S_3 , since otherwise $\text{supp}(\omega_*) = \emptyset$ ($* = X, Y$, see Figures 4.1, 4.2). In such cases the triple point corresponds to one of the Gauss diagrams in Figure 4.3. We say the triple point is of type $(\leftarrow, s_1, s_2, s_3)$ (resp. $(\rightarrow, s_1, s_2, s_3)$) if it corresponds to the left (resp. right) Gauss diagram in Figure 4.3. The arrows “ \leftarrow ” and “ \rightarrow ” indicate the direction of the oriented chord connecting the right-most and the left-most points of the Gauss diagrams.

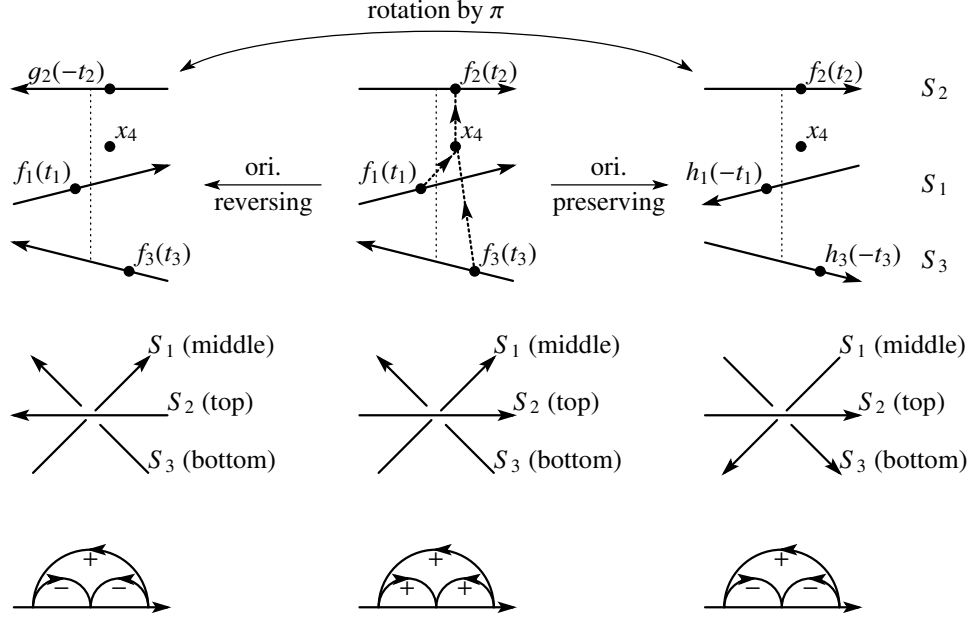


FIGURE 4.4. The case that the triple point is of type $(\leftarrow, +, +, +)$

4.2. **Contribution of triple points to I_Y .** We first consider the case where the triple point is of type $(\leftarrow, s_1, s_2, s_3)$. We parametrize S_k ($k = 1, 2, 3$) by affine maps $f_k: (-\delta, \delta) \rightarrow S_k$ so that the midpoint $f_k(0)$ corresponds to the triple point and the orientations are compatible with the signs s_k . Define the maps $h_{i4}: (-\delta, \delta)^{\times 3} \times \mathbb{R}^3 \rightarrow S^2$ and $h_{42}: (-\delta, \delta)^{\times 3} \times \mathbb{R}^3 \rightarrow S^2$ as indicated by \mathcal{Y} (Figure 3.3). If we put $h_Y := h_{14} \times h_{42} \times h_{34}: (-\delta, \delta)^{\times 3} \times \mathbb{R}^3 \rightarrow S^2$, then the integral

$$(4.1) \quad I_Y^{\leftarrow, s_1, s_2, s_3} := \int_{(-\delta, \delta)^{\times 3} \times \mathbb{R}^3} h_Y^*(\eta \times \eta \times \eta)$$

is the contribution of a triple point of type $(\leftarrow, s_1, s_2, s_3)$ to I_Y .

Lemma 4.1. $I_Y^{\leftarrow, s_1, s_2, s_3} = 0$ for sufficiently small ϵ .

Proof. First note that if we replace

- the parametrization f_2 of S_2 with $g_2(t) := f_2(-t)$, or
- the parametrizations f_1, f_3 of S_1, S_3 respectively with $h_1(t) := f_1(-t)$ and $h_3(t) := f_3(-t)$,

then we obtain models of triple point of type $(\leftarrow, s_1, -s_2, -s_3)$, here $-s_k = \mp$ if $s_k = \pm$ (see Figure 4.4). The resulting models differ from each other by the π -rotation around N , but since we are assuming that η is $O(2)$ -invariant, these models should give the same value $I_Y^{\leftarrow, s_1, -s_2, -s_3}$.

Define two diffeomorphisms $F, G: (-\delta, \delta)^{\times 3} \times \mathbb{R}^3 \rightarrow (-\delta, \delta)^{\times 3} \times \mathbb{R}^3$ respectively by

$$(4.2) \quad F(t_1, t_2, t_3; x_4) := (t_1, -t_2, t_3; x_4) \quad \text{and} \quad G(t_1, t_2, t_3; x_4) := (-t_1, t_2, -t_3; x_4).$$

These diffeomorphisms make the following diagram commutative for both F, G .

$$(4.3) \quad \begin{array}{ccc} (-\delta, \delta)^{\times 3} \times \mathbb{R}^3 & \xrightarrow{h_Y} & (S^2)^{\times 3} \\ \cong \downarrow \star & \nearrow h_{Y, \star} & \\ (-\delta, \delta)^{\times 3} \times \mathbb{R}^3 & & \end{array} \quad (\star = F, G)$$

Here $h_{Y, \star}$ is h_Y defined with f_2 (resp. f_1, f_3) replaced by g_2 (resp. h_1, h_3) if $\star = F$ (resp. $\star = G$). Since F reverses the orientation while G preserves, we have

$$(4.4) \quad I_Y^{\leftarrow, s_1, s_2, s_3} = - \int_{(-\delta, \delta)^{\times 3} \times \mathbb{R}^3} h_{Y, F}^*(\eta \times \eta \times \eta) = + \int_{(-\delta, \delta)^{\times 3} \times \mathbb{R}^3} h_{Y, G}^*(\eta \times \eta \times \eta),$$

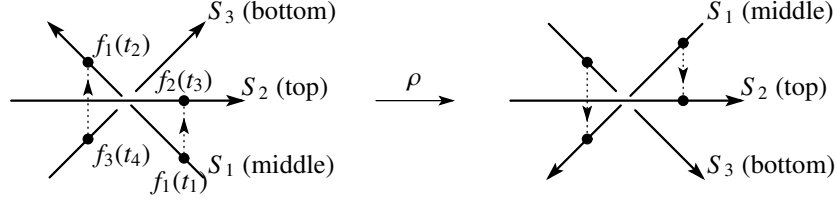


FIGURE 4.5. The case for X'_1 ; the triple point changes its type from $(\leftarrow, -, +, +)$ to $(\leftarrow, +, -, -)$

and

$$(4.5) \quad I_Y^{\leftarrow, s_1, -s_2, -s_3} = \int_{(-\delta, \delta)^3 \times \mathbb{R}^3} h_{Y, \star}^*(\eta \times \eta \times \eta) \quad \text{for both } \star = F, G.$$

Thus, we have $I_Y^{\leftarrow, s_1, s_2, s_3} = I_Y^{\leftarrow, s_1, -s_2, -s_3} = -I_Y^{\leftarrow, s_1, -s_2, -s_3}$. \square

The same holds for $I_Y^{\rightarrow, s_1, s_2, s_3}$. Thus we have proved the following.

Proposition 4.2. $I_Y^{\leftarrow, s_1, s_2, s_3} = I_Y^{\rightarrow, s_1, s_2, s_3} = 0$ for any $s_1, s_2, s_3 \in \{+, -\}$ and sufficiently small $\epsilon > 0$.

As for 3-component long links, we need to investigate the contribution $I_Y^{\leftarrow, s_1, s_2, s_3}$ and $I_Y^{\rightarrow, s_1, s_2, s_3}$ of triple points that involve all the three components. These contributions are similarly defined to (4.1) with S_k ($k = 1, 2, 3$) replaced by segments on the k -th component of the link that form a triple point. The same argument as above shows that $I_Y^{\leftarrow, s_1, s_2, s_3} = I_Y^{\rightarrow, s_1, s_2, s_3} = 0$ for sufficiently small $\epsilon > 0$.

4.3. Contribution of triple points to I_X . Consider the model for a triple point formed by the segments S_1, S_2 and S_3 , as in §4.2. To compute the contribution of the configurations of types X'_1 , suppose that the triple point is of type $(\leftarrow, s_1, s_2, s_3)$ and each S_k is parametrized by an affine map $f_k: (-\delta, \delta) \rightarrow S_k$. Define the maps $h_{13}, h_{42}: (-\delta, \delta)^4 \rightarrow S^2$ as indicated by Figure 4.1 (the left-most), and put $h_{X'_1} = h_{13} \times h_{42}: (-\delta, \delta)^4 \rightarrow (S^2)^{\times 2}$. Then the integral

$$(4.6) \quad I_X^{X'_1, s_1, s_2, s_3} := \int_{(-\delta, \delta)^4} h_{X'_1}^*(\eta \times \eta)$$

is the contributions of configurations of type X'_1 to I_X . In the same ways the contribution I_X^{*, s_1, s_2, s_3} of configurations of type $*$ to I_X , $*$ = $(X'_2, l), (X'_2, r), X'_3$, are defined. For $*$ = (X'_2, r) and X'_3 , we need to assume that the triple point is of type $(\rightarrow, s_1, s_2, s_3)$.

Lemma 4.3. For all $s_1, s_2, s_3 \in \{+, -\}$, we have

- (1) $I_X^{X'_k, s_1, s_2, s_3} = -I_X^{X'_k, s_1, -s_2, -s_3} = I_X^{X'_k, -s_1, -s_2, -s_3}$ ($k = 1, 3$),
- (2) $I_X^{(X'_2, *) , s_1, s_2, s_3} = I_X^{(X'_2, *) , s_1, -s_2, -s_3} = I_X^{(X'_2, *) , -s_1, -s_2, -s_3}$ for both $*$ = l, r ,

where $-s_k = \mp$ for $s_k = \pm$,

Proof. (1) We first prove (1) for X'_1 . Consider the reflection $\rho: \mathbb{R}^3 \rightarrow \mathbb{R}^3$ with respect to the plane that contains $\mathbb{R}N$ and S_2 (see Figure 4.5). Then $\rho \circ f_k$ ($k = 1, 2, 3$) form the model for the triple point of type $(\leftarrow, -s_1, -s_2, -s_3)$. Define $\varphi: (S^2)^{\times 2} \rightarrow (S^2)^{\times 2}$ by $\varphi := \rho \times \rho$. Then we have a commutative diagram

$$(4.7) \quad \begin{array}{ccc} (-\delta, \delta)^4 & \xrightarrow{h_{X'_1}} & (S^2)^{\times 2} \\ & \searrow \widehat{h}_{X'_1} & \downarrow \varphi \\ & & (S^2)^{\times 2} \end{array}$$

here $\widehat{h}_{X'_1}$ is $h_{X'_1}$ defined with f_k replaced by $\rho \circ f_k$. This proves $I_X^{X'_1, s_1, s_2, s_3} = I_X^{X'_1, -s_1, -s_2, -s_3}$, since φ preserves the orientation and we assume that η is $O(2)$ -invariant.

Let $g_k: (-\delta, \delta) \rightarrow S_k$ ($k = 1, 3$) be the parametrizations of S_k with opposite orientation, namely $g_k(t) := f_k(-t)$. If f_1, f_2, f_3 form a triple point of type $(\leftarrow, s_1, s_2, s_3)$, then g_1, f_2, g_3 form a triple point of type $(\leftarrow, s_1, -s_2, -s_3)$ (see Figure 4.6). Define $F: (-\delta, \delta)^4 \rightarrow (-\delta, \delta)^4$ by $F(t_1, \dots, t_4) := (-t_1, -t_2, t_3, -t_4)$, then we have a commutative

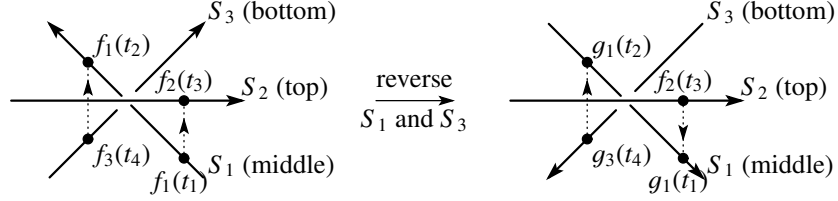


FIGURE 4.6. The case for X'_1 ; the triple point changes its type from $(\leftarrow, -, +, +)$ to $(\leftarrow, -, -, -)$

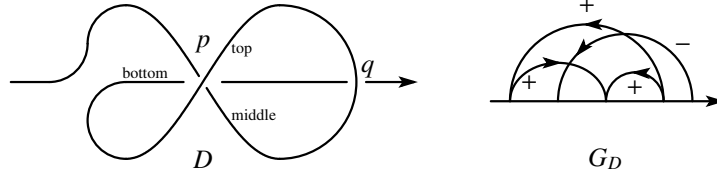


FIGURE 4.7. The long knot f ; the triple point is of type $(\leftarrow, +, +, +)$ and $\langle X, G_D \rangle = 1 \cdot (-1) = -1$

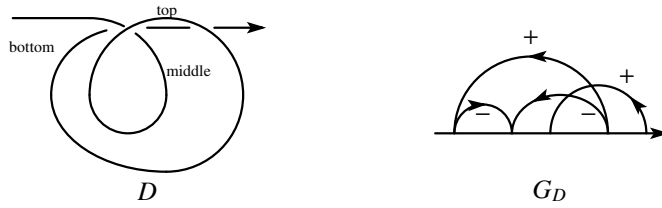


FIGURE 4.8. The long knot g ; the triple point is of type $(\leftarrow, +, -, -)$ and $\langle X, G_D \rangle = 0$

diagram

$$(4.8) \quad \begin{array}{ccc} (-\delta, \delta)^{\times 4} & \xrightarrow{h_{X'_1}} & (S^2)^{\times 2} \\ F \downarrow & \nearrow \underline{h}_{X'_1} & \\ (-\delta, \delta)^{\times 4} & & \end{array}$$

here $\underline{h}^{X'_1}$ is $h^{X'_1}$ defined with f_1, f_3 replaced respectively by g_1, g_3 . This proves $I_X^{X'_1, s_1, s_2, s_3} = -I_X^{X'_1, s_1, -s_2, -s_3}$, since F reverses the orientation.

The proof of (1) for X'_3 is the same, replacing F with $G(t_1, \dots, t_4) = (-t_1, t_2, -t_3, -t_4)$.

(2) The proof of $I_X^{(X'_2, *), s_1, s_2, s_3} = I_X^{(X'_2, *), -s_1, -s_2, -s_3}$ is the same as (1). That of $I_X^{(X'_2, *), s_1, s_2, s_3} = I_X^{(X'_2, *), s_1, -s_2, -s_3}$ is also similar to (1), but we need to replace F and G with $H(t_1, \dots, t_4) = (-t_1, t_2, t_3, -t_4)$, that preserves orientations. \square

Consider the long knot f shown in Figure 4.7. Clearly f is isotopic to the unknot, and hence $c(f) = 0$. G_D is as in Figure 4.7. For sufficiently small $\epsilon > 0$, we have $I_X(f) - I_Y(f) = I_X(f)$ by Proposition 4.2. There exists one pair of double crossings that contributes to $I_X(f)$ as $\langle X, G_D \rangle = -1$; one double crossing is formed by the bottom and the top segment of p , and the other is q . In addition, because p is a triple point of type $(\leftarrow, +, +, +)$, the contributions of types X'_1 and (X'_2, l) occur. Thus we see that

$$(4.9) \quad 0 = c(f) = \langle X, G_D \rangle + I_X^{X'_1, +, +, +} + I_X^{(X'_2, l), +, +, +} = -1 + I_X^{X'_1, +, +, +} + I_X^{(X'_2, l), +, +, +}.$$

Consider the long knot g shown in Figure 4.8. Clearly g is isotopic to the unknot, and hence $c(g) = 0$. G_D is as in Figure 4.8. In this case the triple point is of type $(\leftarrow, +, -, -)$, and similar to the above, we have

$$(4.10) \quad 0 = c(g) = \langle X, G_D \rangle + I_X^{X'_1, +, -, -} + I_X^{(X'_2, l), +, -, -} = I_X^{X'_1, +, -, -} + I_X^{(X'_2, l), +, -, -}.$$

By (4.9), (4.10) and Lemma 4.3, we have

$$(4.11) \quad I_X^{X'_1, +, +, +} = -I_X^{X'_1, +, -, -} = \frac{1}{2}, \quad I_X^{(X'_2, l), +, +, +} = I_X^{(X'_2, l), +, -, -} = \frac{1}{2}.$$

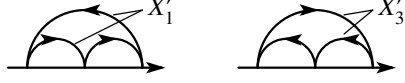


FIGURE 4.9. Subdiagrams that never appear in A_D

Lemma 4.3 and (4.11) show

$$(4.12) \quad I_X^{X'_1, s_1, s_2, s_3} = \frac{s_1 s_2}{2}, \quad I_X^{(X'_2, l), s_1, s_2, s_3} = I_X^{(X'_2, r), s_1, s_2, s_3} = \frac{s_2 s_3}{2}, \quad I_X^{X'_3, s_1, s_2, s_3} = \frac{s_3 s_1}{2}.$$

4.4. **Proof of (2.4) and (2.8).** Let f be a long knot with a diagram D . We may suppose that the subarcs of f near triple or more multiple crossings are parallel to N^\perp like as S_k 's in §4.1. By Proposition 4.2, we only need to compute $I_X(f)$ for sufficiently small $\epsilon > 0$.

As we see in §3.4, every pair $(\alpha, \beta) \in C_X^2(D)$ (Definition 2.3) contributes to I_X by $\text{sgn}(p)\text{sgn}(q)$, where p, q are the double crossings of D corresponding respectively to α and β . Such contributions amount to $\langle X, G_D \rangle$.

Figure 4.1 and (4.12) imply that every triple point of type $(\leftarrow, s_1, s_2, s_3)$ (resp. $(\rightarrow, s_1, s_2, s_3)$) contributes to I_X by $s_1 s_2 / 2 + s_2 s_3 / 2$ (resp. $s_3 s_1 / 2 + s_2 s_3 / 2$). Since A_D never contains subdiagrams shown in Figure 4.9, the contributions of type X'_1 (resp. X'_3) necessarily come from a triple point of type $(\leftarrow, s_1, s_2, s_3)$ (resp. $(\rightarrow, s_1, s_2, s_3)$). Hence these contributions amount to

$$(4.13) \quad \begin{aligned} & \frac{1}{2} \sum_{s_1, s_2, s_3 \in \{+, -\}} \sum_{\text{triple points of type } (\leftarrow, s_1, s_2, s_3)} (s_1 s_2 + s_2 s_3) + \frac{1}{2} \sum_{s_1, s_2, s_3 \in \{+, -\}} \sum_{\text{triple points of type } (\rightarrow, s_1, s_2, s_3)} (s_3 s_1 + s_2 s_3) \\ &= \frac{1}{2} \sum_{(\alpha, \beta) \in C_{X'_1}^2(D)} s_1 s_2 + \frac{1}{2} \sum_{(\alpha, \beta) \in C_{X'_2}^2(D)} s_2 s_3 + \frac{1}{2} \sum_{(\alpha, \beta) \in C_{X'_3}^2(D)} s_3 s_1 = \frac{1}{2} (\langle X'_1, G_D \rangle + \langle X'_2, G_D \rangle + \langle X'_3, G_D \rangle). \end{aligned}$$

This completes the proof of (2.4).

For 3-component links, we can deduce (2.8) by the same argument, just replacing the segments S_k with those on the k -th component.

REFERENCES

1. D. Altschuler and L. Freidel, *Vassiliev knot invariants and Chern-Simons perturbation theory to all orders*, Comm. Math. Phys. **187** (1997), no. 2, 261–287.
2. S. Axelrod and I. M. Singer, *Chern-Simons perturbation theory II*, J. Diff. Geom. **39** (1994), 173–213.
3. R. Bott and C. Taubes, *On the self-linking of knots*, J. Math. Phys. **35** (1994), no. 10, 5247–5287.
4. R. Brooks and R. Komendarczyk, *From integrals to combinatorial formulas of finite type invariants - a case study*, J. Knot Theory Ramifications **33** (2024), no. 8.
5. A. Cattaneo, P. Cotta-Ramusino, and R. Longoni, *Configuration spaces and Vassiliev classes in any dimensions*, Algebr. Geom. Topol. **2** (2002), 949–1000.
6. T. Kohno, *Vassiliev invariants and de Rham complex on the space of knots*, Symplectic geometry and quantization (Sanda and Yokohama, 1993), Contemp. Math., vol. 179, pp. 123–138.
7. R. Koytcheff, *The Milnor triple linking number of string links by cut-and-paste topology*, Alg. Geom. Topol. **14** (2014), 1205–1247.
8. R. Koytcheff, B. Munson, and I. Volić, *Configuration space integrals and the cohomology of the space of homotopy string links*, J. Knot Theory Ramifications **22** (2013), no. 11, 1350061, 73.
9. M. Polyak and O. Viro, *Gauss diagram formulas for Vassiliev invariants*, Internat. Math. Res. Notices (1994), no. 11, 445–453.
10. ———, *On the Casson knot invariant*, J. Knot Theory Ramifications **10** (2001), no. 5, 711–738, Knots in Hellas '98, Vol. 3 (Delphi).
11. K. Sakai, *Lin-Wang type formula for the Haefliger invariant*, Homology Homotopy Appl. **17** (2015), no. 2, 317–341.
12. K. Sakai and T. Watanabe, *1-loop graphs and configuration space integral for embedding spaces*, Math. Proc. Cambridge Phil. Soc. **152** (2012), no. 3, 497–533.
13. I. Volić, *A survey of Bott-Taubes integration*, J. Knot Theory Ramifications **16** (2007), no. 1, 1–42.
14. T. Watanabe, *Configuration space integral for long n -knots and the Alexander polynomial*, Algebr. Geom. Topol. **7** (2007), 47–92.

FACULTY OF MATHEMATICS, SHINSHU UNIVERSITY, 3-1-1 ASAHI, MATSUMOTO, NAGANO 390-8621, JAPAN

Email address: 23ss103j@gmail.com

Email address: sakaik@shinshu-u.ac.jp